

On the luminosity function of galaxies in groups in the Sloan Digital Sky Survey

Ariel Zandivarez, Héctor J. Martínez and Manuel E. Merchán

Grupo de Investigaciones en Astronomía Teórica y Experimental (IATE)
Observatorio Astronómico, Universidad Nacional de Córdoba,
Laprida 854, X5000BGR, Córdoba, Argentina

Consejo Nacional de Investigaciones Científicas y Técnicas (CONICET),
Avenida Rivadavia 1917, C1033AAJ, Buenos Aires, Argentina

arielz@mail.oac.uncor.edu, julian@mail.oac.uncor.edu,
 manuel@mail.oac.uncor.edu

ABSTRACT

Using galaxy groups identified in the Fourth Data Release of the Sloan Digital Sky Survey (SDSS), we compute the luminosity function for several subsamples of galaxies in groups. In all cases, the luminosity functions are well described by Schechter functions, down to the faintest magnitudes we probe, $M_{0.1r} - 5 \log(h) \sim -16$. For the general luminosity function of galaxies in groups in the five SDSS bands, we observe that the characteristic magnitude is brighter in ~ 0.5 magnitudes compared to those obtained for field galaxies by Blanton et al. (2003b). Even when the observed faint end slope is steeper in galaxy groups, it is statistically comparable with the field value. We analyze the dependence of the galaxy luminosity function with system masses finding two clear trends: a continuous brightening of the characteristic magnitude and a steepening of the faint end slope as mass increases. The results in $^{0.1}g$, $^{0.1}r$, $^{0.1}i$ and $^{0.1}z$ bands show the same behavior. Using the $u-r$ color to split the galaxy sample into red and blue galaxies, we show that the changes observed as a function of the system mass are mainly seen in the red, passively evolving, galaxy population, while the luminosities of blue galaxies remain almost unchanged with mass. Finally, we observe that groups having an important luminosity difference between the two brightest galaxies of a system show a steeper faint end slope than the other groups. Our results can be interpreted in terms of galaxy mergers as the main driving force behind galaxy evolution in groups.

Subject headings: galaxies: clusters: general - galaxies: luminosity function - galaxies: statistics.

1. Introduction

To understand the processes that govern galaxy formation and evolution, detailed information must be collected about the behavior of the different galaxy populations under different conditions. A common and useful way to achieve this, is the study of galaxy luminosities and their variation with the environment. The most suitable statistical tool to perform this kind of analysis is the luminosity function (LF) of galaxies. This function describes the distribution of luminosities of a given population of galaxies and, in most cases, it can be parametrized by a function with two parameters excluding the normalization (Schechter 1976), the characteristic absolute magnitude M^* and the faint end slope α . The results obtained from the analysis of these parameters are among the most interesting issues in extragalactic astronomy.

Prior to 2000 the LF has been computed for galaxies in the field, groups and in clusters of galaxies (see for instance Marzke, Huchra & Geller 1994; Lin et al. 1996; Zucca 1997; López-Cruz et al. 1997; Valotto et al. 1997; Ratcliffe et al. 1998; Muriel, Valotto & Lambas 1998; Rauzy, Adami & Mazure 1998; Trentham 1998). Two lines of thought have arisen from these works: one of them states that the LF depends on the environment while the other supports the idea of an universal LF. The dependence of the LF with the environment was proposed by some authors due to the very steep faint end slope found for the LF in clusters of galaxies which was interpreted as an excess of dwarf galaxies relative to the field. Nevertheless, in order to have more reliable results on this matter, large samples of galaxies with high quality photometric and spectroscopic information were needed.

Since the advent of the large surveys of galaxies, such as the Sloan Digital Sky Survey (York et al. 2000) and the Two degree Field Galaxy Redshift Survey (2dFGRS, Colless et al. 2001), much better determinations of the LF have been obtained (Blanton et al. 2001, 2003b, 2005; Norberg et al. 2002; Madgwick et al. 2002; Trentham & Tully 2002; Martínez et al. 2002b; Christlein & Zabludoff 2003; Eke et al. 2004b). Most of these works agree with a flat LF of galaxies in the field ($\alpha \sim -1$) meanwhile a brighter characteristic magnitude M^* and a steeper faint end slope α have been found in galaxy systems. Analyzing a sample of rich clusters of galaxies obtained from a cross-correlation between the Sloan Digital Sky Survey and the Rosat All Sky Survey, Popesso et al. (2005) have found that the very faint end slope ($M_r - 5 \log(h) > -17$) is remarkably steep ($\alpha \sim -2$) on these environments. Similar results have been found by González et al. (2005) when lower density environments as galaxy groups are analyzed. It should be noted that both works have been carried out using statistical background subtraction methods owing to the lack of spectroscopic information for faint galaxies. These methods are sensitive to the background computation (Popesso et al. 2005, see their Table 2) and to the presence of structures along the line of sight (Valotto et al.

2001), therefore, they are less reliable than those based only upon spectroscopic information.

Groups of galaxies are very interesting objects in the universe, since they are the most common systems of galaxies and the evolution of galaxies inside them plays an important role at early stages of cluster galaxies evolution. How important is the variation of galaxy luminosities with the main physical properties of these systems? How does the environment affect the different galaxy populations? Large statistical samples of galaxy groups are needed in order to these questions be addressed.

The largest galaxy redshift survey at the present is the Fourth Data Release of the Sloan Digital Sky Survey (hereafter DR4; Adelman-McCarthy et al. 2005). This catalog covers a very wide area on the sky, has high quality information in five broadbands and comprises two times the number of galaxies in the current Final Release of the 2dFGRS. The huge size of the Sloan galaxy catalog will provide us of the largest galaxy group catalog at the present with very important photometric and spectroscopic information.

The main purpose of this work is to compute the LFs of galaxies in groups under different conditions in order to understand the behavior of galaxies in intermediate density environments and consequently provide important clues on galaxy formation and evolution.

The layout of this paper is as follows. In section 2 we describe the galaxy sample and the group identification. The full analysis of LFs as a function of the band, mass ranges, color and the brightest galaxy is in section 3. Finally in section 4 we summarize and discuss the results.

2. Sample

The Sloan Digital Sky Survey (SDSS) has validated and made publicly available its Fourth Data Release (DR4; Adelman-McCarthy et al. 2005) which is a photometric and spectroscopic survey constructed with a dedicated 2.5 m telescope at Apache Point Observatory in New Mexico. The SDSS DR4 consists of 6670 deg² of five-band, $u g r i z$, imaging data and 673,280 (4783 deg²) spectra of galaxies, quasars and stars. The DR4 Main Galaxy Sample (MGS; Strauss et al. 2002) includes roughly 400,000 galaxies with redshift measurements up to $z \sim 0.3$ and an upper apparent magnitude limit of 17.77 in the r band.

Galaxy groups used in this work have been identified in the MGS of DR4 using the same procedure as in Merchán & Zandivarez (2005). The method consists in using a friend-of-friend algorithm similar to that developed by Huchra & Geller (1982). The algorithm links galaxies (i, j) which satisfy that $D_{ij} \leq D_0 R(z)$ and $V_{ij} \leq V_0 R(z)$ where D_{ij} is the projected

distance and V_{ij} is the line-of-sight velocity difference. The scaling factor $R(z)$ is introduced in order to take into account the decrement of the galaxy number density due to the apparent magnitude limit cutoff (see eq. 5 in Huchra & Geller 1982). We have adopted a transversal linking length D_0 corresponding to an overdensity of $\delta\rho/\rho = 80$, a line-of-sight linking length of $V_0 = 200 \text{ km s}^{-1}$ and a fiducial distance of $10 \text{ } h^{-1}\text{Mpc}$. As in Merchán & Zandivarez (2005), we have also carried out an improvement of the rich group identification. This improvement consists in performing a second identification on galaxy groups with at least ten members in order to split merged systems or to eliminate spurious member detections. This second identification uses a higher density contrast, $\delta\rho/\rho \sim 315$, which produces a more reliable group identification (see Díaz et al. 2005). Group center locations for these groups have been improved using an iterative procedure developed by Díaz et al. (2005). The procedure defines a new group center estimation by using the projected local number density of each member galaxy for weighting their group center distances, and then iterates this estimation by removing galaxies beyond a given distance. The iteration follows until the center location remains unchanged. Since the method needs to compute the projected local number density with five galaxies, this procedure can only be applied to group with at least ten members.

Finally, the group sample comprises 14004 groups with at least 4 members, adding up to 85728 galaxies. Mean properties of groups in this sample are similar to those of the DR3 group catalog as quoted by Merchán & Zandivarez (2005). We obtain a median velocity dispersion, virial mass and radius of 232 km s^{-1} , $3.9 \times 10^{13} \text{ } h^{-1} \mathcal{M}_{\odot}$, and $1.11 \text{ } h^{-1}\text{Mpc}$ respectively.

The magnitudes we use in this work are the Petrosian ones, and have been corrected for Galactic extinction following Schlegel et al. (1998). Absolute magnitudes have been computed assuming $\Omega_0 = 0.3$, $\Omega_{\Lambda} = 0.7$ and a Hubble constant $H_0 = 100 \text{ } h \text{ km s}^{-1} \text{ Mpc}^{-1}$, and K -corrected using the method of Blanton et al. (2003a)¹. We have adopted a band shift to a redshift 0.1, i.e. to approximately the mean redshift of the Main Galaxy Sample of SDSS, as suggested by Blanton et al. (2003a). We have also included evolution corrections to this redshift for each galaxy of the form $(z - 0.1)Q$ where Q varies with the band: 4.22, 2.04, 1.62, 1.61 and 0.76 for u , g , r , i , z bands respectively (Blanton et al. 2003b). Throughout this work we will refer to these shifted bands as $^{0.1}u$ $^{0.1}g$ $^{0.1}r$ $^{0.1}i$ $^{0.1}z$. All magnitudes are in the AB system.

¹kcorrect version 4.1

3. Luminosity function of galaxies in groups

Following the comparative study of different luminosity function estimators by Willmer (1997), we have chosen two methods for computing luminosity functions: the non-parametric C^- method (Lynden-Bell 1971; Choloniewski 1987) and the STY method (Sandage, Tammann & Yahil 1979) for fitting Schechter function parameters. Among the non-parametric methods, the C^- is the most robust estimator, being less affected by different values of the faint end slope of the Schechter parametrization and sample size. Meanwhile, the STY is reliable for fitting analytic expressions without binning the data.

Since we are only interested in studying the LF shape for different subsamples of galaxies in groups, all LFs in this paper are shown in arbitrary units.

3.1. The luminosity function in the SDSS bands

For computing luminosity functions, we have adopted the same apparent magnitude cut-offs as in Blanton et al. (2003b). Given that K -corrections in each band are reliable only in a given redshift range, we have also introduced redshift cut-offs depending on the band (Table 1, see Blanton et al. 2003a).

The $^{0.1}r$ band LF for galaxies in groups is shown in Figure 1, along with the best Schechter function fit. The LF for the other bands and the corresponding fits are displayed in Figure 2. Best fit Schechter parameters can be found in Table 1. It is noticeable from these figures that Schechter functions provide a good description of the LF for all bands.

When comparing our results with those of Blanton et al. (2003b) (their Table 2) for the LFs of all galaxies in DR1’s MGS, we observe that, with the exception of the $^{0.1}u$ band, the characteristic magnitudes, $M^* - 5 \log(h)$ are brighter for galaxies in groups. These observed brightening of M^* ranges from 0.29 in the $^{0.1}z$ band to ~ 0.5 magnitudes in the $^{0.1}g$, $^{0.1}r$ and $^{0.1}i$, with more than 7σ significance in all cases. At the same time, group galaxies show a small steepening of the faint end slope, α . The steepening is more pronounced for bluer bands, $^{0.1}u$, $^{0.1}g$, where a change of ~ 0.2 in α is observed. Nevertheless, these differences are not very significant, since all of them lie within $\sim 2\sigma$. These results are in agreement with those obtained by Martínez et al. (2002b) for galaxies in groups identified in the 100K release of the 2dFGRS, in the b_J band. They found that the characteristic magnitude is brighter for galaxies in groups respect to the LF obtained for field galaxies by Norberg et al. (2002), while the faint end slope for galaxies in groups was statistically comparable with the field value.

In hierarchical models for galaxy formation and evolution, the frequency of mergers increase in intermediate mass systems such as groups. Therefore, in this scenario, galaxies in groups and clusters are expected to be typically brighter than in the field, resulting in a brighter M^* . This could explain the differences between group and field galaxies. On the other hand, the $^{0.1}u$ band result, is not unexpected since this band is closely related to the current star formation, and galaxies in systems are likely to have lower or suppressed star formation rates (see for instance Martínez et al. 2002a).

3.2. The group mass dependence of the galaxy LF

In this subsection we study how the LF depends on group masses. A previous analysis on this matter was done by Eke et al. (2004b) using the 2dFGRS Percolation-Inferred Galaxy Group catalog (2PIGG; Eke et al. 2004a). They split their group sample into three mass bins and compute the corresponding LFs using the standard $1/V_{\text{max}}$ and the STY methods. Though their high mass bin is statistically poor and does not follow the same trend as the lower mass ones, they conclude that M^* and α decrease when mass increases.

Given the large number of groups we have identified in DR4, we expect to obtain a more detailed description on this subject. We have split the full sample of $z \leq 0.22$ groups into 6 mass bins defined to have roughly the same number of groups (~ 2200). The details of this selection can be seen in Table 2. The large number of galaxies in the samples allows the determination of LFs with a high level of confidence, even when we are splitting the sample into several bins.

In Figure 3 we show the resulting $^{0.1}r$ band LF for each mass bin. As it can be seen from Figure 3, the LFs are well fitted by Schechter functions for all masses (see parameters in Table 2). In order to simplify the reader interpretation of the results, we show the values of M^* *vs.* α (Figure 4) and M^* and α as a function of the mass (Figure 5). Figure 4 displays the 1σ and 2σ confidence ellipses according to STY computations. Y-axis error-bars in Figure 5 are the projections of the 1σ joint error ellipse onto each axis of Figure 4, while x-axis error-bars are the semi-interquartile range of the median mass. There are two clear and continuous trends: a brightening of M^* and a simultaneous steepening of α as mass increases. M^* changes in ~ 0.75 magnitudes while α varies in 0.4, over two orders of magnitude in group mass. We have done the same calculations for the other SDSS bands. The best-fitting Schechter parameters are in Table 3. We found the same global trends in all bands, with some differences for the $^{0.1}u$ band. In this case we observe a brightening of M^* of ~ 0.4 magnitudes, significantly smaller than the ~ 0.75 magnitudes value for the other bands. This is not unexpected, since the $^{0.1}u$ band is sensitive to star formation, i.e., $^{0.1}u$

luminosity function is a poor indicator of the underlying mass distribution. The faint end slope variation with mass is roughly the same, ~ 0.5 , for all bands.

A similar result was found by Croton et al. (2005) analysing the variation of the of the LFs of galaxies in the 2dFGRS with the environment. They study the dependence of the LFs with the density contrast estimated within $8h^{-1}\text{Mpc}$ sphere observing a smooth variation of the Schechter parameters in density environments ranging from voids to clusters. It should be taken into account that this parameter can not be directly related with group masses since the virial mass describes a closer environment than the corresponding to $8h^{-1}\text{Mpc}$ density contrast, even so, their results shows the same trends than the described in the previous paragraph.

Our results means that, as system mass increases, the characteristic luminosity of galaxies increases. Regarding the steepening of the faint end slope with mass, at least two possibilities arise: an important fraction of bright, $M_{0.1r} \lesssim -18$, galaxies gets brighter, then the ‘knee’ of the Schechter function becomes less pronounced and this gives a steeper α , or, there are some physical mechanisms that increase the number of faint, $M_{0.1r} \gtrsim -18$, galaxies. Therefore, there exist some processes that enhance galaxy brightness for bright galaxies and possibly some other processes that increase the number of faint galaxies. The effect of these processes becomes more noticeable for massive systems. Merging and galactic cannibalism are likely to be responsible of producing brighter galaxies. As the result of a tidal interaction between two galaxies, the massive counterpart can get brighter while the less massive diminishes its luminosity. On the other hand, processes involving the interaction between galaxies and the intra-system environment, such as ram pressure, are important for massive systems. It results in the loss of gas in less bound galaxies, drastically reducing the star formation.

3.3. The LF for the Red and Blue sequences in groups

In a previous work, Strateva et al. (2001) found that the color distribution of galaxies can be approximated by a bimodal function, i.e. by the sum of two normal Gaussian functions. This behavior can be explained by two different formation processes which generate two galaxy populations with different average colors. The most common choice is to adopt the $u - r$ color to split the galaxy distribution into two different populations. There are several works in the literature that use this color distribution to distinguish between two galaxy populations. Recently, Baldry et al. (2004) have shown that it can not be chosen an unique color divider point since this point depends on absolute magnitude. So, in order to divide the sample of galaxies in groups into two different populations we have parametrized the

relation between the color divider point and the absolute magnitude in the $^{0.1}r$ band. To do so, we firstly use the MGS and split it into absolute magnitude bins of width 0.5. For each absolute magnitude bin, we fit to the $K + E$ -corrected $^{0.1}(u - r)$ color distribution the sum of two Gaussian functions. The color divider point is estimated as the intersection point between both Gaussian functions. Finally, we fit a straight line to the color divider points as a function of the $^{0.1}r$ absolute magnitude. The resulting linear relation is

$$C_{\text{cut}}(M_{0.1r}) = -0.062(M_{0.1r} + 18) + 2.078. \quad (1)$$

Figure 6 shows the $1/V_{\text{max}}$ weighted color-magnitude distribution for the MGS. The straight line shows the color divider point as a function of absolute magnitude according to Equation 1. Using this function we split the sample of galaxies in groups into two subsamples of Red, $^{0.1}(u - r) > C_{\text{cut}}(M_{0.1r})$, and Blue, $^{0.1}(u - r) < C_{\text{cut}}(M_{0.1r})$, galaxies.

The $^{0.1}r$ band LFs for the Red and Blue sequences of galaxies in groups are shown in Figure 7 together with the respective Schechter best-fitting parameters (see also Table 4). When comparing our results with field values by Baldry et al. (2004), we observe that the Red sequence in groups has a brighter characteristic magnitude and a slightly steeper faint end slope. Taking into account error-bars and the band shift, the Red sequence in the field and in groups have comparable LFs. On the other hand, there are some differences between the Blue sequence in the field and in groups. We find a brighter M^* and a steeper α in groups. Baldry et al. (2004) find $M_r^* - 5 \log(h) = -19.82 \pm 0.08$ for the Blue sequence, which means a difference of ~ 0.8 magnitudes in M^* . The Blue sequence faint end slope is $\alpha = -1.35 \pm 0.05$, therefore, galaxies in groups have a steeper α in ~ 0.12 . Nevertheless, owing to the errors in both determinations, the faint end slopes are statistically comparable ($\sim 1.5 \sigma$ difference). It should be noted that the similarity between the results obtained for field and group galaxies in the Red sequence it is not unexpected since these galaxies are mainly located in galaxy systems. On the other hand, we do expect a difference for the LF of the Blue sequence in groups compared with that obtained in the field, since a large fraction of Blue galaxies are not in groups and, consequently, do not suffer the action of some typical physical processes of dense environments.

We have also computed the $^{0.1}r$ band LF for Blue and Red sequences as a function of group mass, splitting groups into the same six mass bins used in the previous subsection. The resulting LFs are shown in Figure 8 while the corresponding best-fitting Schechter parameters are quoted in Table 4 and shown in Figure 9. In the later, upper panel shows the behavior of M^* as a function of mass, meanwhile the lower panel displays α as a function of mass. We also show in both panels the variation of the Schechter parameters with mass for all galaxies in groups, computed in the previous subsection. Regarding the variation of M^* with mass, it is clear that the change is larger for the Red sequence. M^* smoothly decreases in ~ 1.1

magnitudes between the lowest and the highest mass subsamples. For the Blue sequence, M^* shows a small variation (~ 0.2 magnitudes) for the first 5 mass bins, and doubles this brightening in the last one. The faint end slope as a function of mass also shows a larger variation for the Red sequence, a steepening of 0.75 from low to high mass. Excluding the highest mass bin ($\alpha \sim -1.6$), the Blue sequence has a constant value of $\alpha \sim -1.4$.

According to our results, the Red sequence luminosities show a strong variation with the system mass, while the Blue sequence luminosities are roughly independent of mass. In the previous subsection we found that M^* brightens and α steepens when system mass increases, hence we can now conclude that those changes are mainly observed in one of the populations, the Red one.

3.4. The influence of the brightest galaxy

When studying clusters of galaxies, one of the most interesting subjects is the Brightest Cluster Galaxy (BCG). They are preferentially elliptical, are located in the center of the potential well and are particularly massive and bright. Even though their evolution and the effect of the environment upon them are not well understood, the most plausible scenario for their origin is that they form rapidly from mergers of several galaxies during the early stages of cluster or group collapse. Later, they become brighter in more massive systems as hierarchical structure formation continues (Merritt 1985; Edge 1991; Dubinski 1998; Lin & Mohr 2004).

In this subsection we are interested in studying the LF of groups (i.e. low and intermediate mass systems) where there is an important luminosity difference between the brightest group galaxy (BGG) and the second ranked galaxy. To do so, we have split the sample of groups into two subsamples with roughly the same number of groups: those with a magnitude difference between the BGG and the second ranked galaxy, $\Delta M_{12} \geq 0.6$, and those with $\Delta M_{12} < 0.6$. It is worth to be mentioned that the absolute magnitude distribution of the BGGs for both subsamples are quite similar. In order to avoid any possible bias with redshift we have restricted the group subsamples to $0.02 \leq z \leq 0.05$. The resulting luminosity functions are shown in Figure 10 and the corresponding best-fitting Schechter parameters are in Table 5. For the $\Delta M_{12} \geq 0.6$ subsample M^* is ~ 0.7 magnitudes brighter, and α is ~ 0.3 steeper with $\sim 5\sigma$ significance, than the $\Delta M_{12} < 0.6$ subsample values. The two subsamples have similar group mass distributions. This was also found by Lin & Mohr (2004) in clusters, where the difference in luminosity between the BCG and the second ranked galaxy do not correlate with mass. Hence, the results above, can not be associated with a possible mass bias.

As said above, the most likely scenario for the BCGs formation is based upon the idea that these objects have been formed from mergers between several galaxies that take place in groups or low mass cluster. Under this scheme, the merging galaxies that form the BCGs are the BGGs, i.e. the more luminous galaxies in groups. Since the merger rate is a decreasing function of the velocity dispersion of a galaxy system, mergers should be the main responsible for the formation of the BGGs, progenitors of the future BCG. From our results, we conclude that BGGs that are considerably brighter than the remaining group members, are preferentially found in groups where mergers have been more effective, producing a brightening of the characteristic magnitude M^* . Moreover, it is known that the galactic cannibalism solely at the present epoch is unlikely to be the process responsible for the BGG origin since this scenario is not in agreement with a high value of ΔM_{12} (Merritt 1985; Tremaine 1990). Loh & Strauss (2006) have observed that the large values of ΔM_{12} measured around the Luminous Red Galaxies in the SDSS support the idea that the BCGs form during the system collapse due to the process of merging small structures with a subsequent growth due to the accretion of lesser members. Therefore, we can add to our picture that the BGGs of our subsample with larger values of ΔM_{12} went through merging processes at the early stages of the galaxy systems formation.

4. Summary and discussion

In this work we have studied the behavior of galaxy luminosities in groups of galaxies. We use the largest sample of galaxy groups at the present which allow us to obtain very reliable statistical results. The groups are identified in the SDSS DR4 using the same procedure as the described by Merchán & Zandivarez (2005). The galaxy luminosities analysis is performed computing the LF for several subsamples of galaxies in groups. Our results can be summarized as follows:

- First, we compute the LFs of galaxies in groups in different SDSS bands. Our results show that, except for the $^{0.1}u$ band, the characteristic magnitude, M^* , is ~ 0.5 magnitudes brighter than the obtained for field galaxies by Blanton et al. (2003b). The faint end slope, α , of these LFs are slightly steeper than their field counterparts.
- Then, we study the dependence of the $^{0.1}r$ LF of galaxies in groups for different bins in group mass. We observe two clear trends: a brightening of the characteristic magnitude ($\Delta M^* \sim 0.75$) and a steepening of the faint end slope ($\Delta \alpha \sim 0.4$) as mass increases.
- Similar results are found when analyzing the mass dependence of the LFs in the remaining SDSS bands for both, M^* and α . Only the $^{0.1}u$ band shows a less pronounced

brightening in the characteristic magnitude. Since the $^{0.1}u$ band is more sensitive to current galaxy star formation, we expect that the LFs in this band to be less suitable to trace the mass, i.e., to show the real brightening of M^* as a function of group mass as observed in the other bands.

- We made use of the bimodal $^{0.1}(u - r)$ distribution to split the galaxy sample into a Red and a Blue sequence. The divider point among the populations is estimated from a linear relation as a function of the $^{0.1}r$ absolute magnitude. The LF obtained for the Red sequence is quite similar to that obtained by Baldry et al. (2004) for field galaxies. On the other hand, even when the Blue sequence in groups shows a similar faint end slope than the observed for the Blue sequence in the field, its characteristic magnitude is significantly brighter than the field counterpart.
- Regarding the dependence of Red and Blue sequence LF in groups with the group mass we observe that the Red sequence shows stronger changes in both, the characteristic magnitude and the faint end slope. The behavior of the Blue sequence remains almost unchanged as system mass increases.
- Finally, studying the effect of the brightest group galaxy on these environments we split the galaxy sample into two subsamples: groups with ($\Delta M_{12} \geq 0.6$) and without ($\Delta M_{12} < 0.6$) a remarkable luminosity difference between the brightest group galaxy and the second ranked galaxy. We observe that those groups with larger ΔM_{12} have a brighter M^* and a steeper α than the other group subsample.

The most plausible scenario to explain the results above is one in which mergers have played a fundamental role in galaxy evolution in groups. It is well known from the literature that galaxy mergers are more frequent in low mass systems since the low galaxy velocity dispersion should induce higher encounter rates (Merritt 1985). They can account for the observed brightening of M^* with mass and the reddening of galaxy colors given that these processes could consume gas in a burst of star formation and subsequently, at later times, induce lower star formation rates. Our results fit into the scenario proposed by Baldry et al. (2004) where mergers are the cause of the color bimodality, with a red population resulting from merger processes and a blue population that form stars at a rate determined by their internal physical properties. The fact that the LF of the blue population in groups remains almost unchanged with mass, supports the idea of a population that evolves independently of environment, while the observed behavior in the LF of the red galaxies reveals that these objects have been through major changes due to environmental effects. Recently, Faber et al. (2005) have studied the evolution of the LF of the Red and Blue sequences up to $z \sim 1$ using also the bimodality distribution to perform the distinction among both populations. The

main result is that the number density obtained for Red sequence galaxies shows a strong evolution, while the Blue sequence remains almost unchanged in the sampled redshift range. They conclude that the more plausible scenario to account for this effect is one in which some blue galaxies have suffered a strong suppression of their star formation due to gas-rich mergers, resulting in a migration to the red sequence and subsequently evolving there due to several stellar mergers. The Faber et al. (2005) model is quite consistent with the one suggested here to explain the behaviour of both populations.

Another result that should be explained is the decrease of the faint end slope with group mass. This parameter is the one that describes the shape of the Schechter function and it is defined by both, the faint and the bright ends of the LF. Therefore, any significant variation in any of these regions, should change the value of α . A shallower distribution of bright galaxies can result in a steeper value of α without changing the number of faint galaxies. Hence, the merger scenery can also explain the resulting behavior of α with mass. This does not exclude the possible incidence of environmental processes such as galaxy harassment, ram pressure, etc., that could enhance the number of faint galaxies. Nevertheless, it should be reminded that the limiting apparent magnitude of the MGS does not allow to probe the very faint end of the LF, therefore, the observed change in α with mass, can not be unambiguously associated with a dwarf galaxy population.

Acknowledgments

This work has been partially supported by grants from Consejo de Investigaciones Científicas y Técnicas de la República Argentina (CONICET), the Secretaría de Ciencia y Técnica de la Universidad Nacional de Córdoba (SeCyT), Agencia Nacional de Promoción Científica de la República Argentina and Agencia Córdoba Ciencia.

Funding for the Sloan Digital Sky Survey (SDSS) has been provided by the Alfred P. Sloan Foundation, the Participating Institutions, the National Aeronautics and Space Administration, the National Science Foundation, the U.S. Department of Energy, the Japanese Monbukagakusho, and the Max Planck Society. The SDSS Web site is <http://www.sdss.org/>. The SDSS is managed by the Astrophysical Research Consortium (ARC) for the Participating Institutions. The Participating Institutions are The University of Chicago, Fermilab, the Institute for Advanced Study, the Japan Participation Group, The Johns Hopkins University, the Korean Scientist Group, Los Alamos National Laboratory, the Max Planck Institut für Astronomie (MPIA), the Max Planck Institut für Astrophysik (MPA), New Mexico State University, University of Pittsburgh, University of Portsmouth, Princeton University, the United States Naval Observatory, and the University of Washington.

REFERENCES

- Adelman-McCarthy J.K., et al. (The SDSS Collaboration), 2005, ApJS, in press (astro-ph/0507711).
- Baldry, I. K., Glazebrook, K., Brinkmann, J., Ivezić, Ž., Lupton, R. H., Nichol, R. C., & Szalay, A. S. 2004, ApJ, 600, 681
- Barnes, J. E., & Hernquist, L. 1992, ARA&A, 30, 705
- Blanton, M. R., et al. 2001, AJ, 121, 2358.
- Blanton, M. R., et al. 2003a, AJ, 125, 2348
- Blanton, M. R., et al. 2003b, ApJ, 592, 819
- Blanton, M. R., Lupton, R. H., Schlegel, D. J., Strauss, M. A., Brinkmann, J., Fukugita, M., & Loveday, J. 2005, ApJ, 631, 208
- Choloniewski J., 1987, MNRAS, 226, 273.
- Christlein D., Zabludoff A.I., 2003, ApJ, 591, 764.
- Colless, M., et al. 2001, MNRAS, 328, 1039
- Croton, D. J., et al. 2005, MNRAS, 356, 1155
- Díaz E., Zandivarez A., Merchán M.E., Muriel H. 2005, ApJ, in press.
- Dubinski, J. 1998, ApJ, 502, 141
- Edge, A. C. 1991, MNRAS, 250, 103
- Eke, V. R., et al. 2004a, MNRAS, 348, 866
- Eke, V. R., et al. 2004b, MNRAS, 355, 769
- Faber S. M., et al. 2005, submitted to MNRAS, astro-ph/0506044.
- González R.E., Lares M., Lambas D.G., Valotto C., 2005, A&A submitted, astro-ph/0507144.
- Huchra J.P., Geller M.J., 1982, ApJ, 257, 423.
- Lin H., Kishner R.P., Schectman S.A., Landy S.D., Oemler A., Tucker D.L., Schechter P.L., 1996, ApJ, 464, 60.

- Lin, Y.-T., & Mohr, J. J. 2004, *ApJ*, 617, 879
- Loh Y., Strauss M., 2006, *MNRAS*, 366, 373.
- López-Cruz O., Yee H.K.C., Brown J.P., Jones C., Forman W., 1997, *ApJ*, 475, 97.
- Lynden-Bell D., 1971, *MNRAS*, 155, 95.
- Madgwick, D. S., et al. 2002, *MNRAS*, 333, 133
- Martínez, H. J., Zandivarez, A., Domínguez, M., Merchán, M. E., & Lambas, D. G. 2002a, *MNRAS*, 333, L31
- Martínez, H. J., Zandivarez, A., Merchán, M. E., & Domínguez, M. J. L. 2002b, *MNRAS*, 337, 1441.
- Marzke R.O., Huchra J.P. & Geller M.J., 1994, *ApJ*, 428, 43.
- Merchán M.E., Zandivarez A., 2005, *ApJ*, 630, 759.
- Merritt, D. 1985, *ApJ*, 289, 18
- Muriel H., Valotto C. & Lambas D.G., 1998, *ApJ*, 506, 540.
- Norberg P., et al., 2002, *MNRAS*, 336, 907.
- Popesso, P., Böhringer, H., Romaniello, M., & Voges, W. 2005, *A&A*, 433, 415
- Ratcliffe A., Shanks T., Parker Q.A., Fong R., 1998, *MNRAS*, 294, 147.
- Rauzy S., Adami C. & Mazure A., 1998, *A&A*, 337, 31.
- Sandage A., Tammann G.A., Yahil A., 1979, *ApJ*, 352, 82.
- Schechter P., 1976, *ApJ*, 203, 297.
- Schlegel, D. J., Finkbeiner, D. P., & Davis, M. 1998, *ApJ*, 500, 525
- Strateva I., et al., 2001, *AJ*, 122, 1861.
- Strauss, M. A., et al. 2002, *AJ*, 124, 1810
- Tremaine S., 1990, in *Dynamics and Interaction of Galaxies*, (ed. Wielen R.), Springer Verlag.
- Trentham N., 1998, *MNRAS*, 295, 360.
- Trentham N., Tully R.B., 2002, *MNRAS*, 335, 712.

Valotto C.A., Nicotra M.A., Muriel H., Lambas D.G., 1997, ApJ, 479, 90.

Valotto, C. A., Moore, B., & Lambas, D. G. 2001, ApJ, 546, 157

Willmer C.N.A, 1997, AJ, 114, 898.

York, D. G., et al. 2000, AJ, 120, 1579

Zucca E., et al., 1997, A&A, 326, 477.

Table 1. STY best-fitting Schechter parameters for the luminosity functions of galaxies in groups

Band	m_{lim}	Redshift range	N_{galaxies}	$M^* - 5 \log(h)$	α
$^{0.1}u$	18.40	0.02 – 0.14	15743	-17.83 ± 0.03	-1.13 ± 0.04
$^{0.1}g$	17.70	0.02 – 0.17	37239	-19.71 ± 0.02	-1.09 ± 0.02
$^{0.1}r$	17.77	0.02 – 0.22	83869	-20.85 ± 0.01	-1.08 ± 0.01
$^{0.1}i$	16.91	0.02 – 0.22	54233	-21.21 ± 0.02	-1.15 ± 0.02
$^{0.1}z$	16.50	0.02 – 0.22	46001	-21.47 ± 0.02	-1.12 ± 0.01

Table 2. Group mass dependence of the LF in the $^{0.1}r$ band: STY best-fitting Schechter parameters

Mass sample	Mass range ^a	N_{groups}	N_{galaxies}	$M^* - 5 \log(h)$	α
\mathcal{M}_1	11.0 – 12.9	2322	10326	-20.44 ± 0.04	-0.93 ± 0.03
\mathcal{M}_2	12.9 – 13.3	2392	12514	-20.56 ± 0.04	-0.93 ± 0.03
\mathcal{M}_3	13.3 – 13.6	2409	13580	-20.64 ± 0.04	-0.96 ± 0.03
\mathcal{M}_4	13.6 – 13.9	2362	14415	-20.75 ± 0.04	-1.01 ± 0.03
\mathcal{M}_5	13.9 – 14.25	2150	14626	-20.86 ± 0.04	-1.06 ± 0.04
\mathcal{M}_6	> 14.25	2231	17331	-21.20 ± 0.04	-1.29 ± 0.04

^aUnits are $\log(\mathcal{M}/(h^{-1}M_{\odot}))$

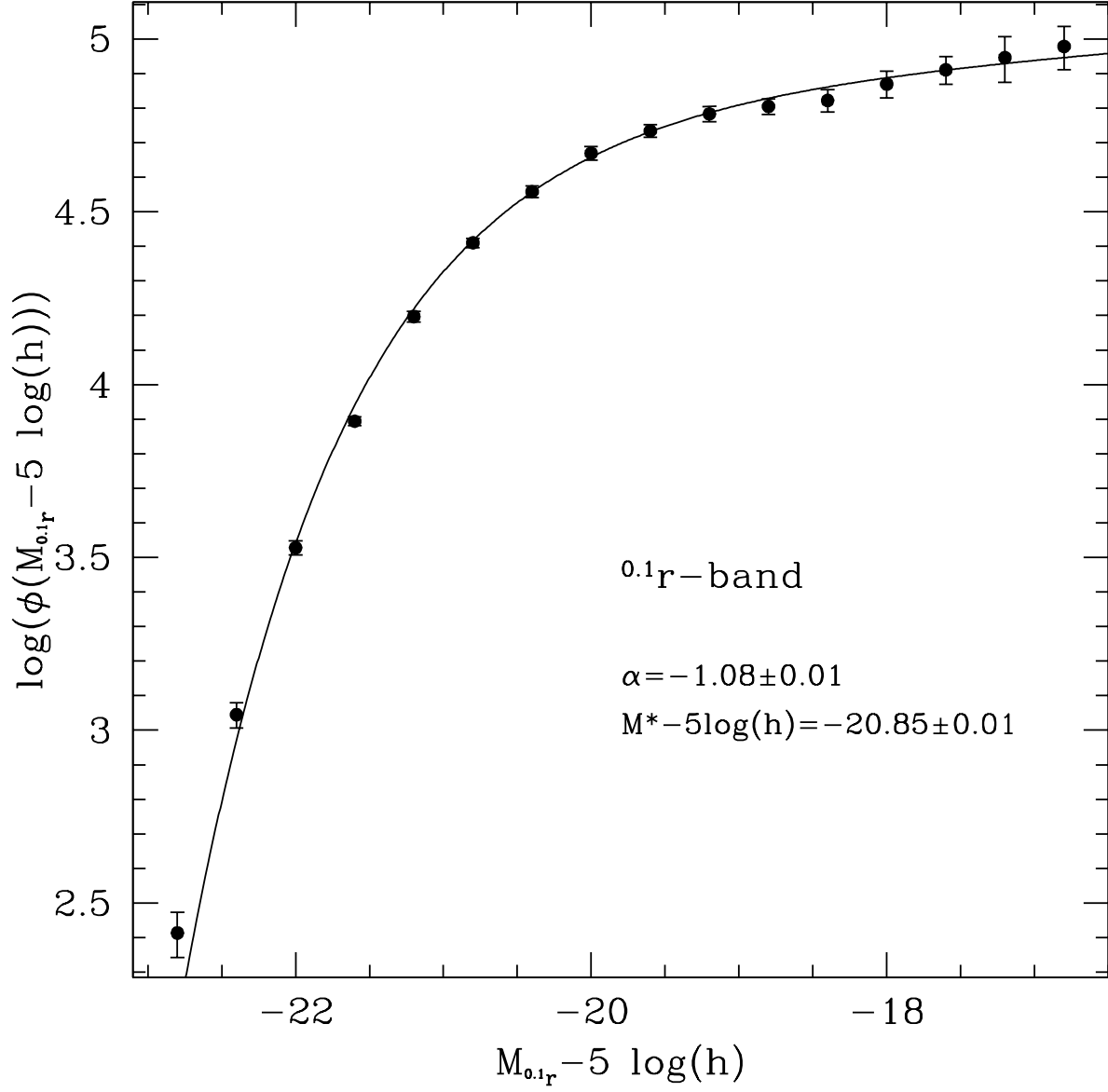


Fig. 1.— The $^{0.1}r$ band luminosity function of galaxies in groups in arbitrary units. Solid line shows the best-fitting Schechter function (see labels). Error bars were computed using the bootstrap resampling technique.

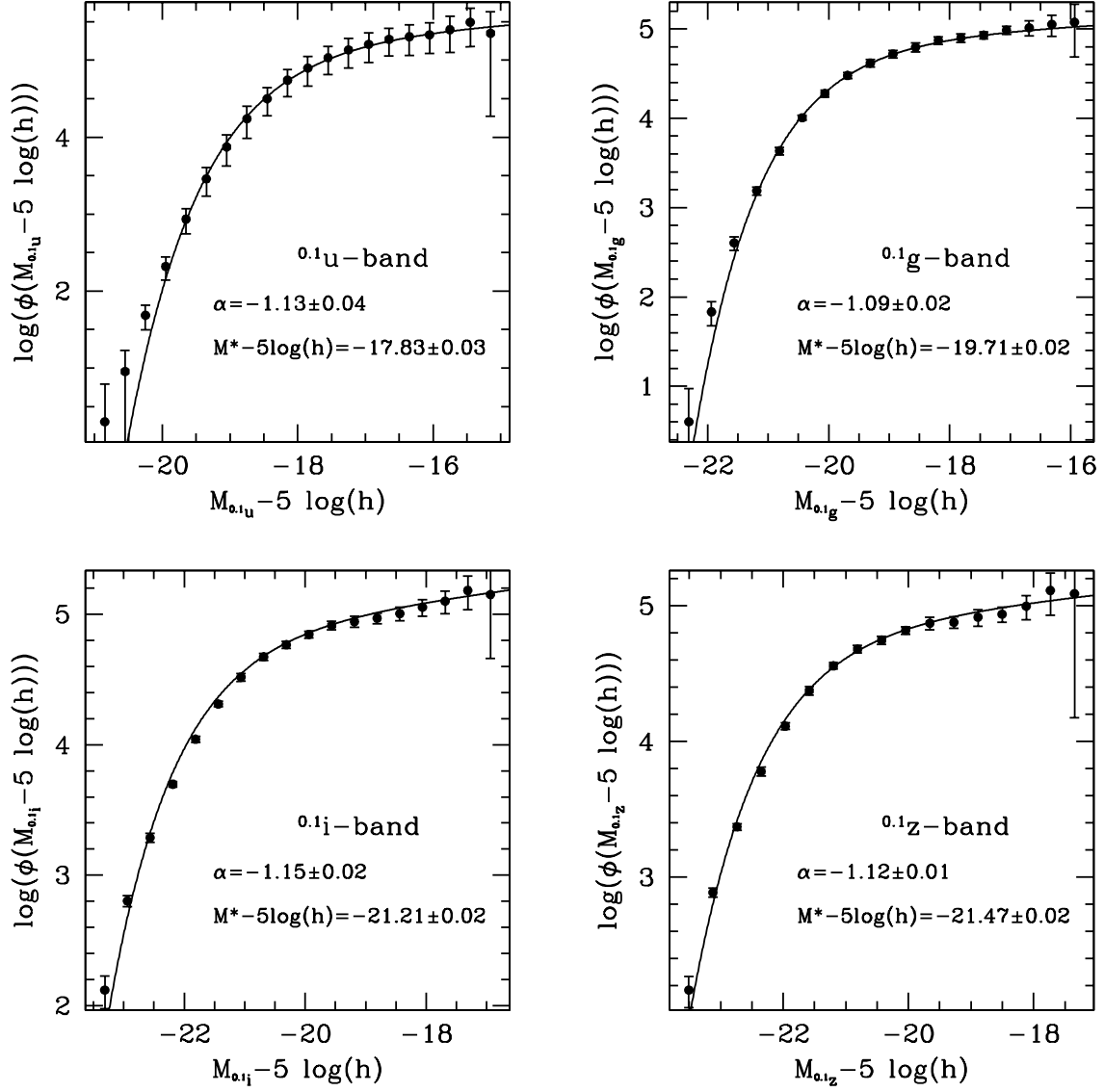


Fig. 2.— Luminosity functions of galaxies in groups in different bands (arbitrary units). Solid lines in each panel show the best-fitting Schechter functions (see labels). Error bars were computed using the bootstrap resampling technique.

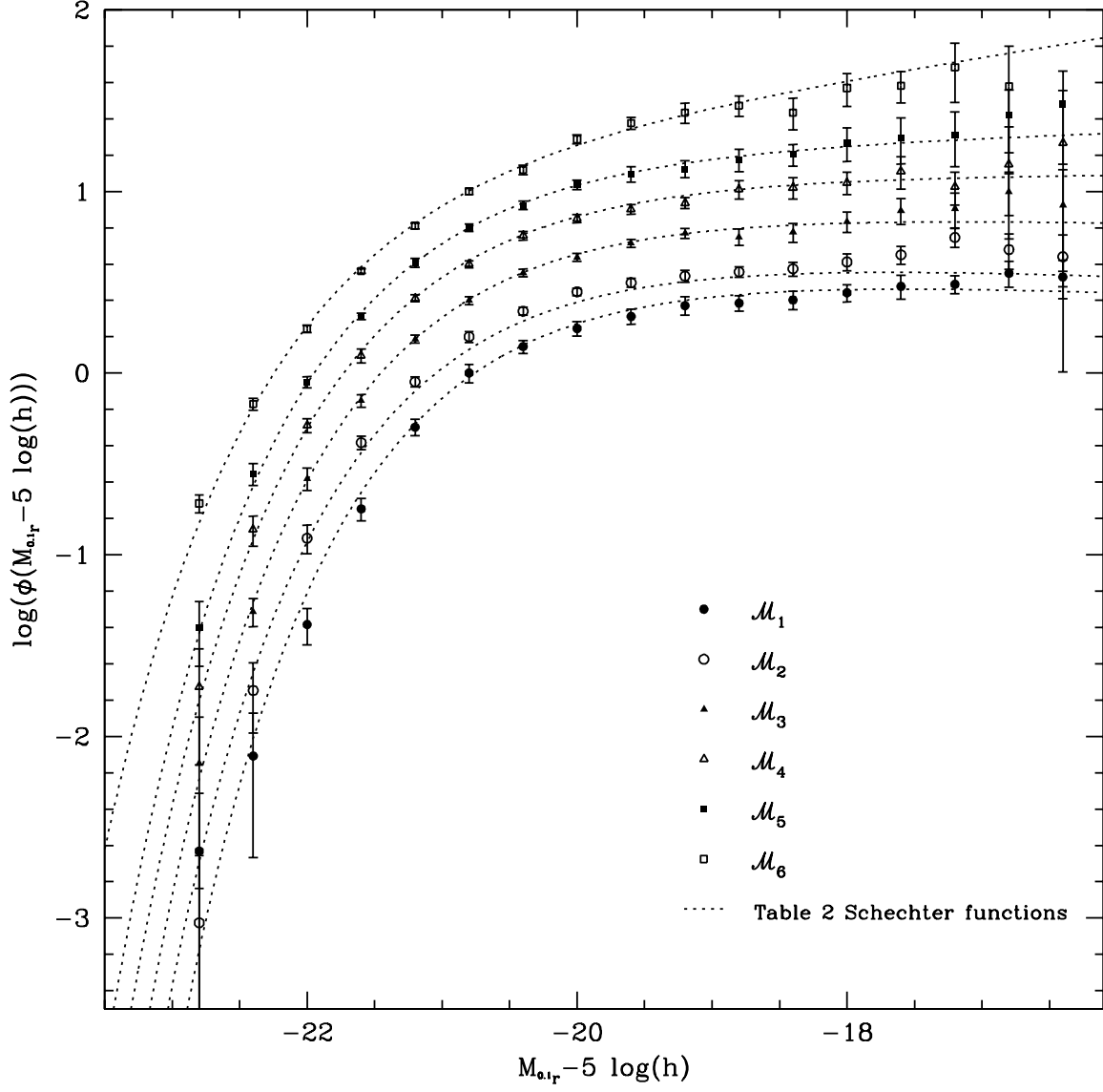


Fig. 3.— $^{0.1}r$ band luminosity functions of galaxies in groups in arbitrary units for different mass ranges (see Table 2). Dotted lines show the best-fitting Schechter functions. Error bars were computed using the bootstrap resampling technique.

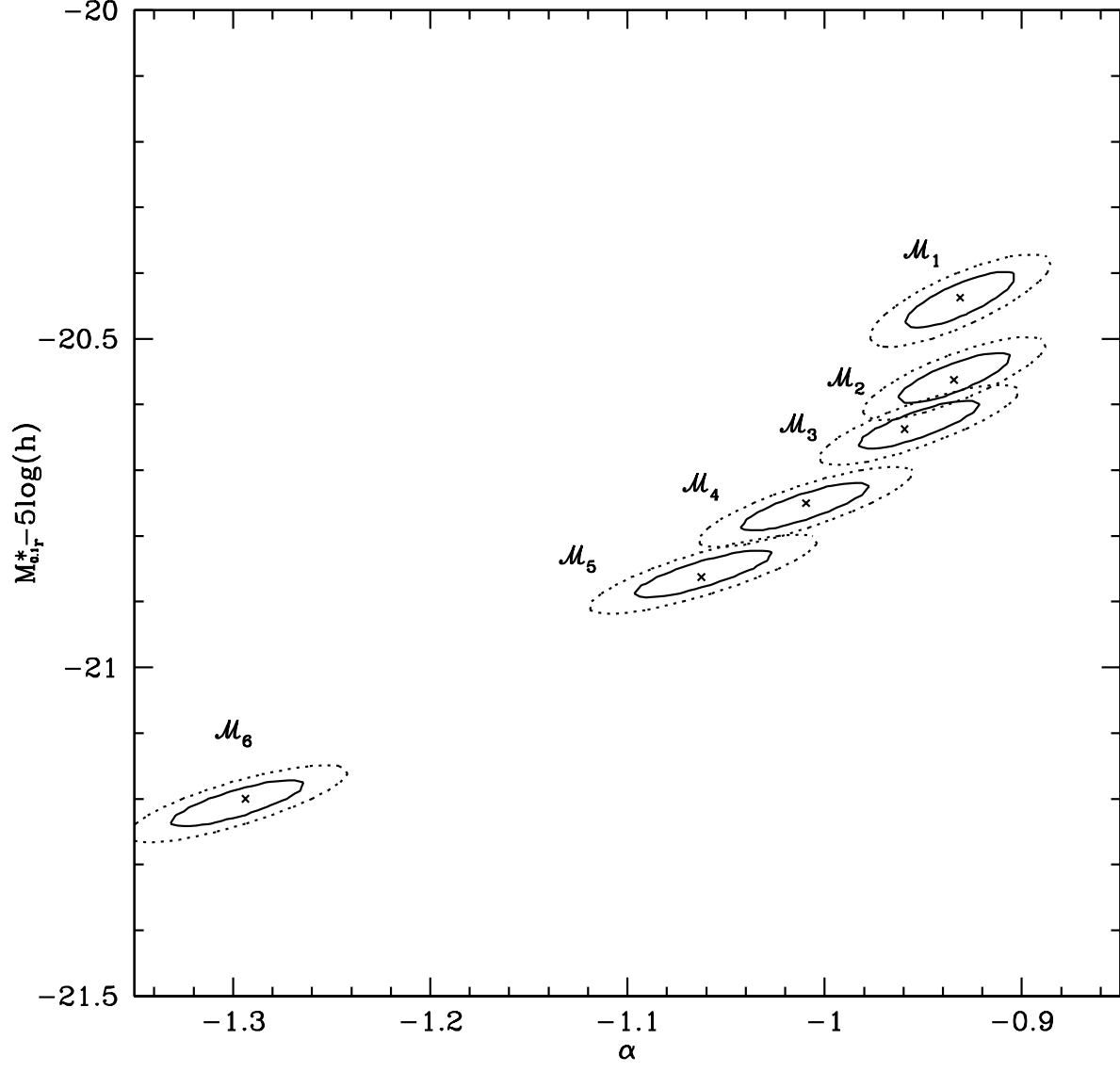


Fig. 4.— The best-fitting Schechter parameters of the $^{0.1}r$ band LF for different mass ranges. The 1σ and 2σ confidence ellipses are also shown.

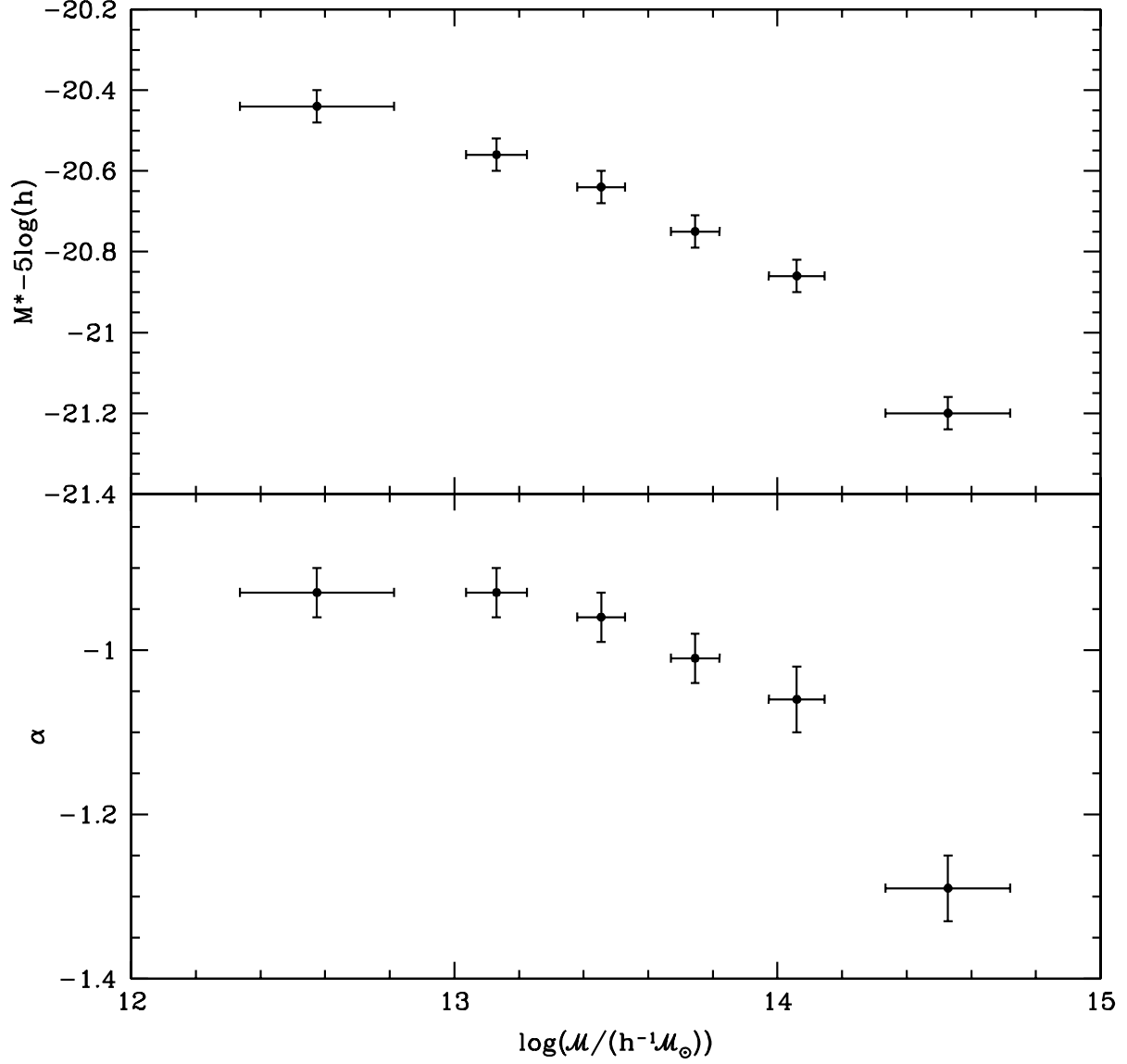


Fig. 5.— The best-fitting Schechter parameters $M^* - 5\log(h)$ (upper panel) and α (lower panel) for the $^{0.1}r$ band LF as a function of the median mass. The mass error bars are the semi-interquartile range, whereas the errors in the Schechter parameters are the projections of 1σ joint error ellipse onto each axis.

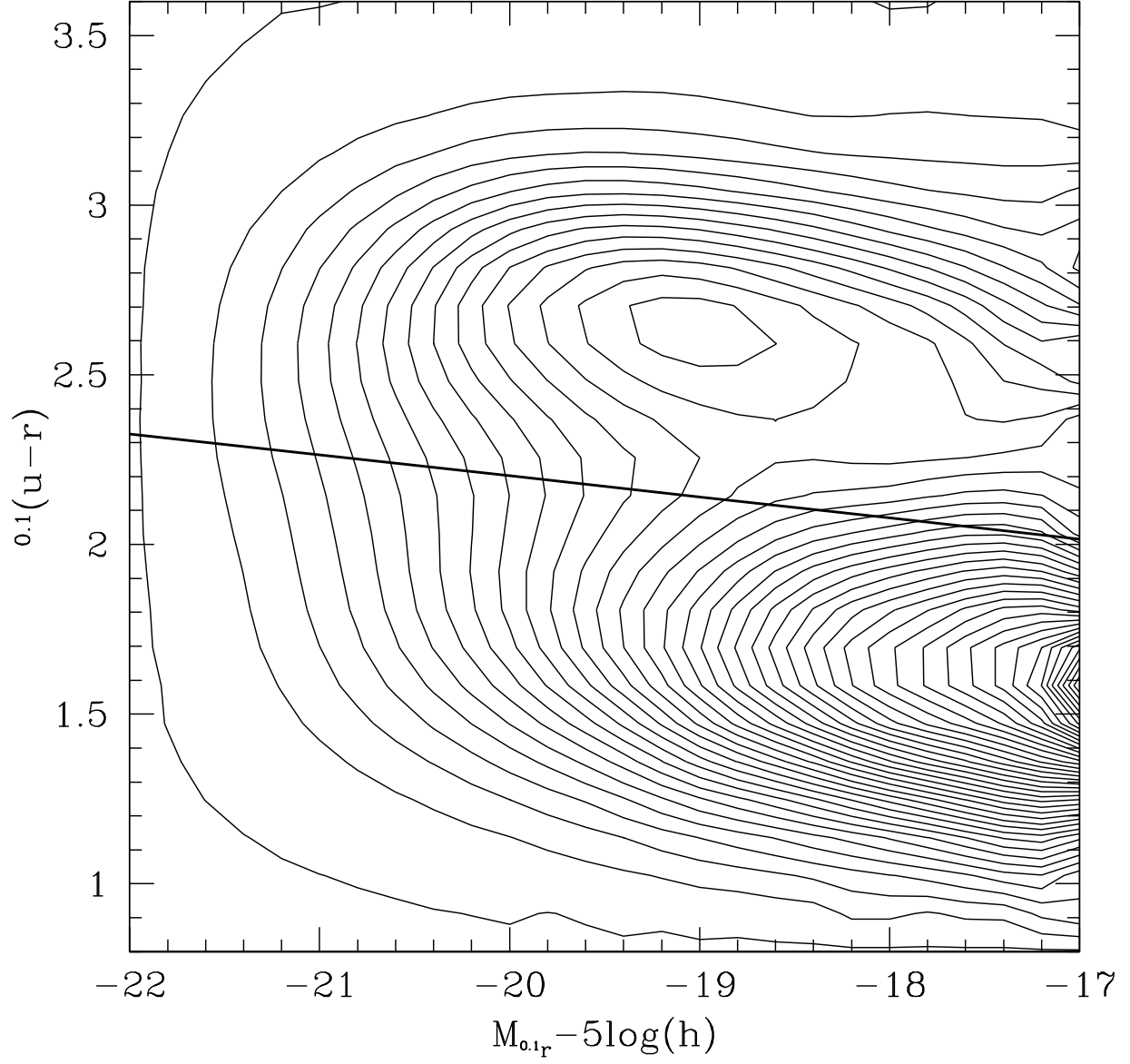


Fig. 6.— Color-magnitude distribution corrected for incompleteness. The contours are on a linear scale in number density. The thick straight line is the divider point of the bimodal distribution (see Equation 1).

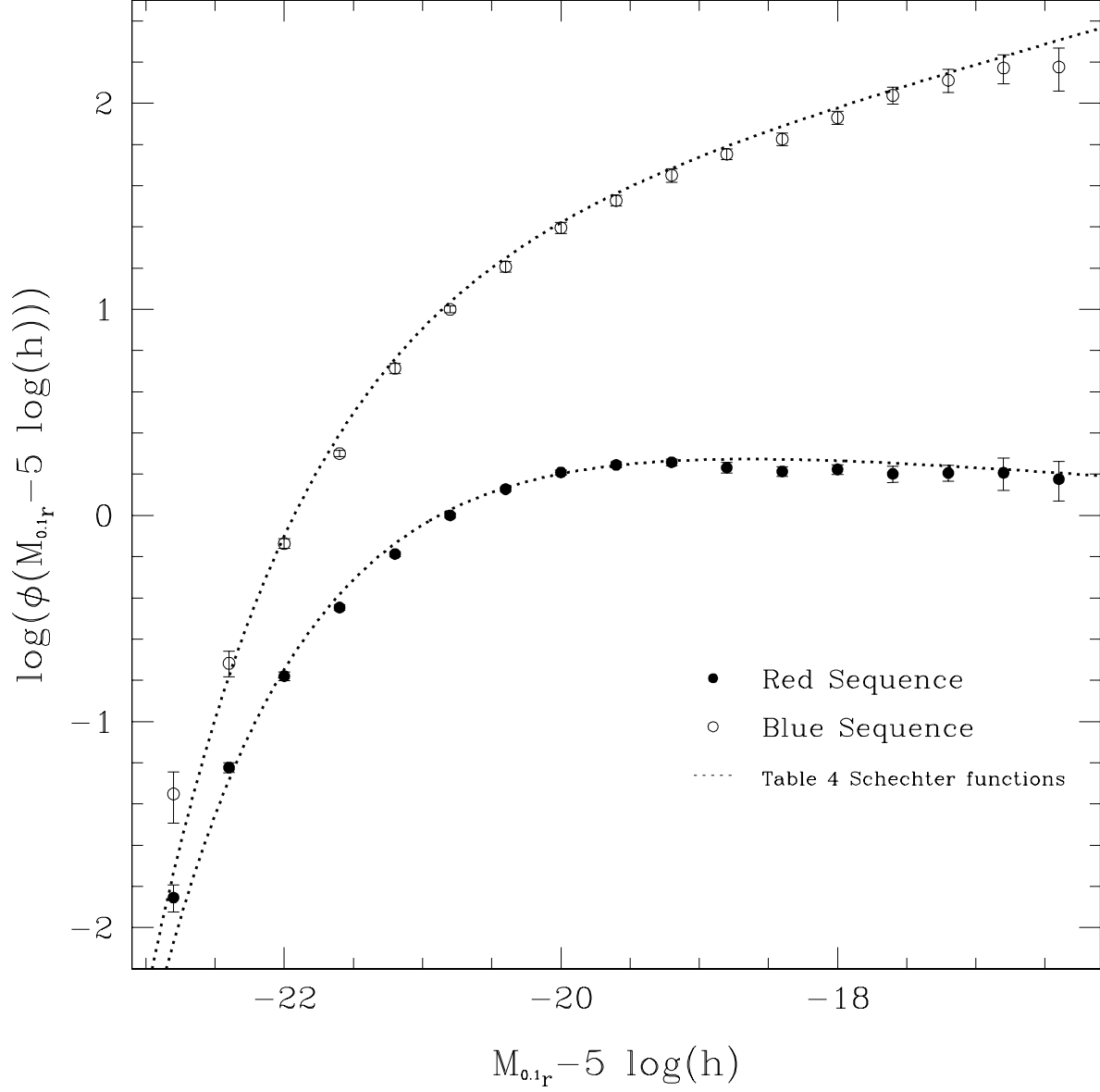


Fig. 7.— $^{0.1r}$ band luminosity function of the Red (upper panel) and Blue (lower panel) sequences in groups in arbitrary units. Dotted lines show the best-fitting Schechter functions. Error bars are computed using a bootstrapping technique.

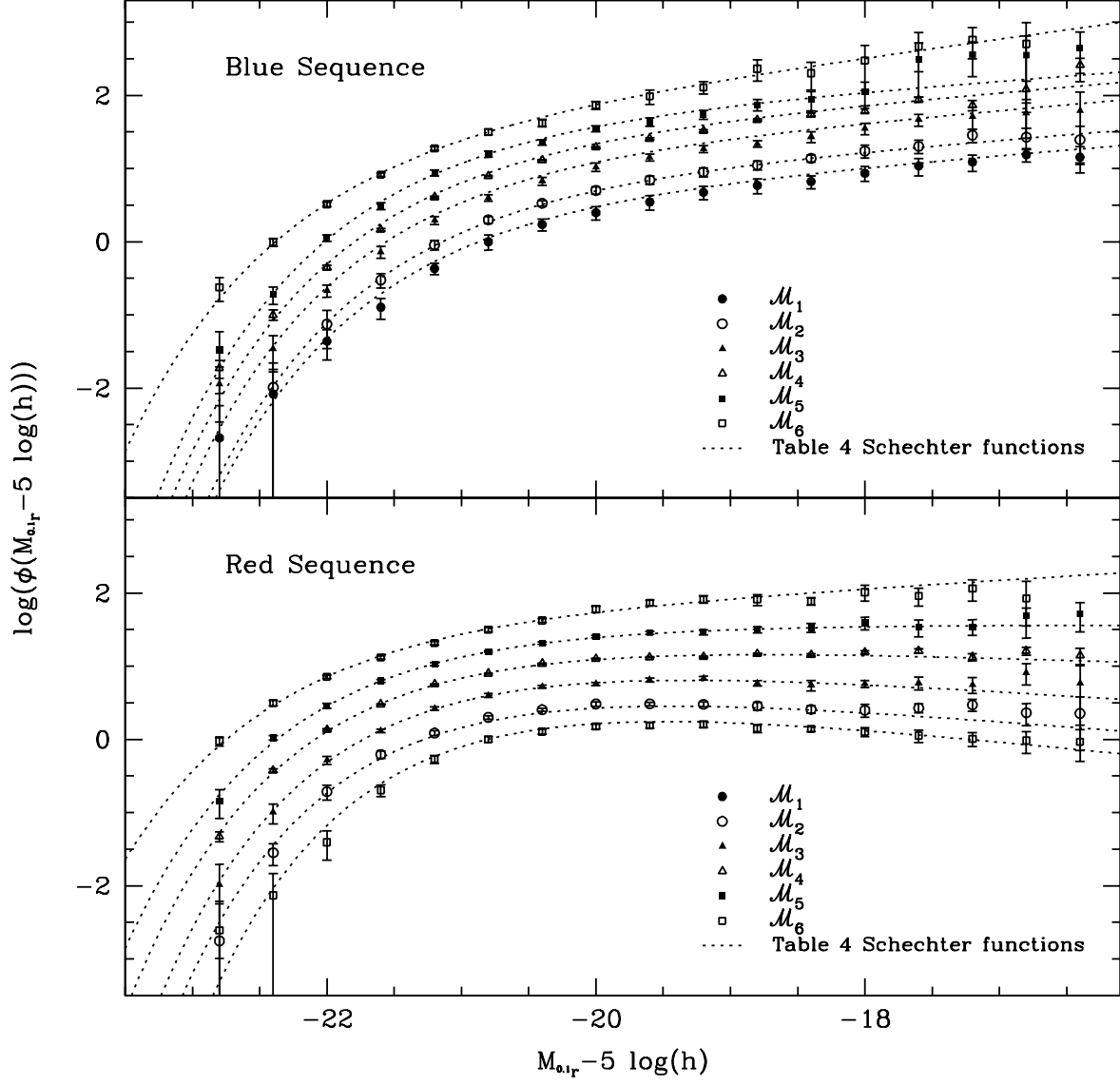


Fig. 8.— $^{0.1r}$ band luminosity function of the Red (upper panel) and Blue (lower panel) sequences in groups for different group mass ranges (arbitrary units). Dotted lines show the best-fitting Schechter functions. Error bars are computed using a bootstrapping technique.

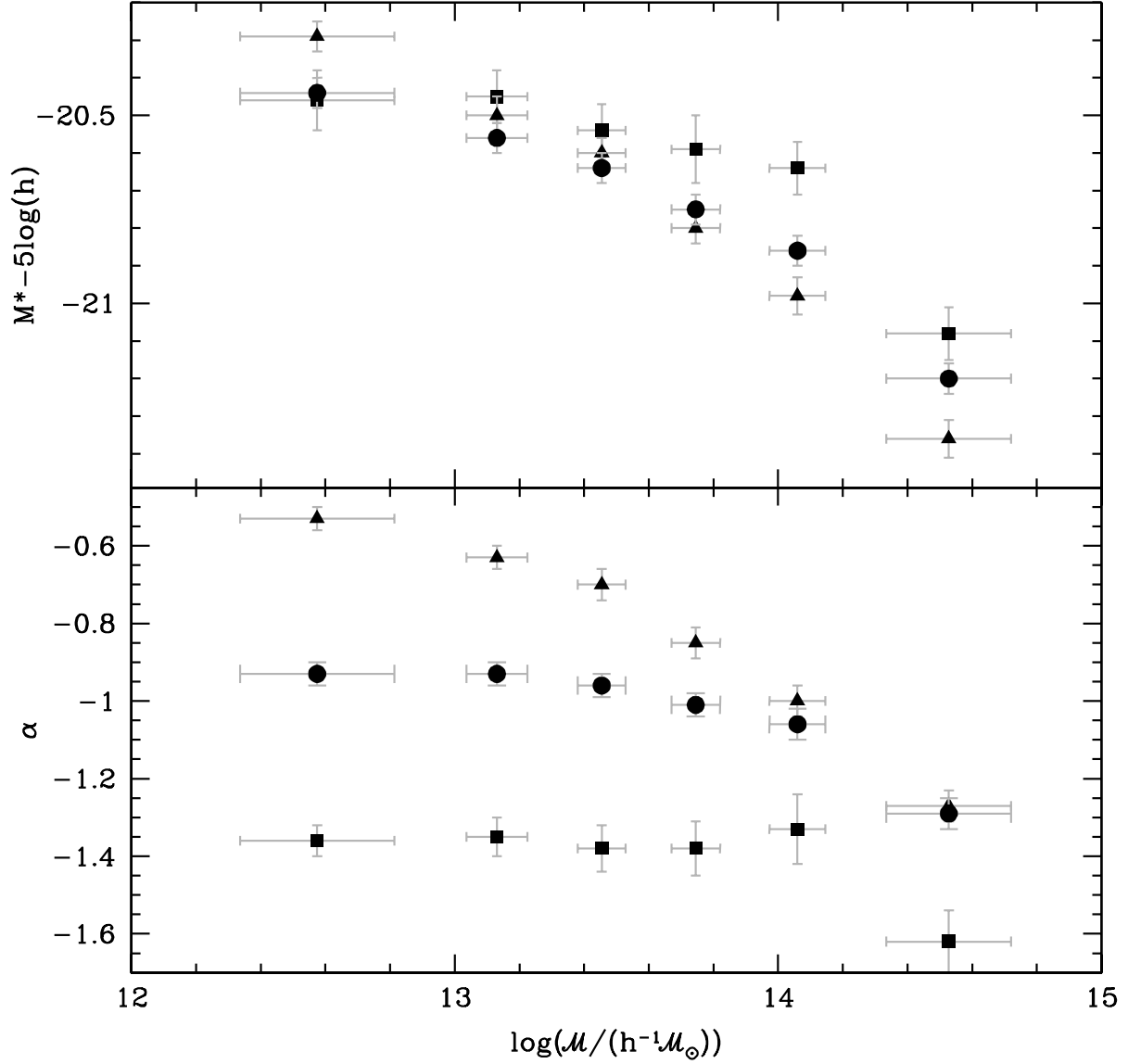


Fig. 9.— The best-fitting Schechter parameters for the $^{0.1}r$ band LF of red (triangles) and blue (squares) galaxies in groups as a function of the median mass of a given range. The mass error bars are the semi-interquartile range, whereas the errors in the Schechter parameters are the projections of 1σ joint error ellipse onto each axis. Circles are the best-fitting Schechter parameters for the whole sample of galaxies in groups in each mass range as plotted in Figure 5.

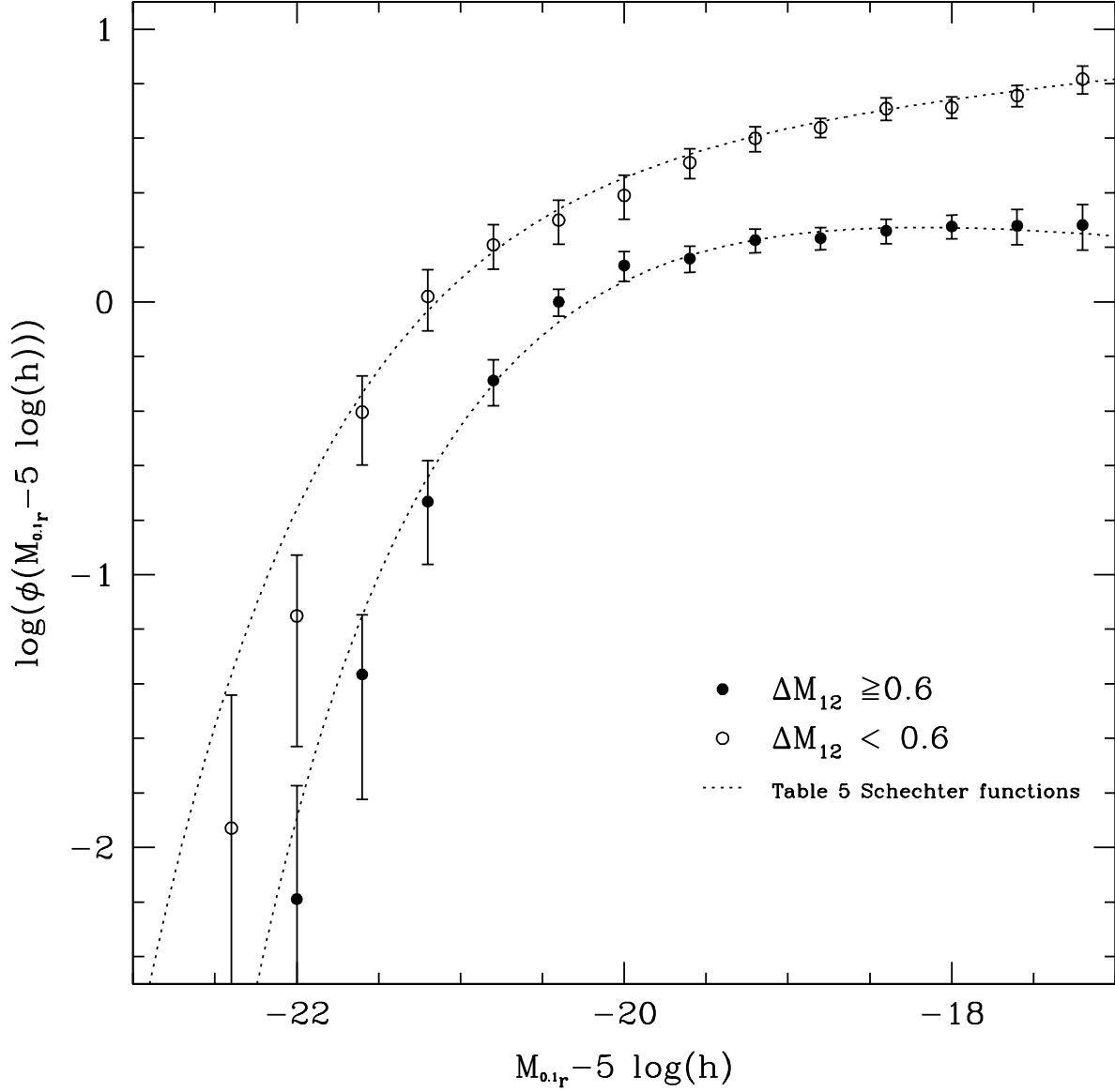


Fig. 10.— $^{0.1}r$ band luminosity functions of galaxies in groups for samples with absolute magnitude difference between the first and second brightest galaxies ΔM_{12} greater or equal than 0.6 (upper panel) and lesser than 0.6 (lower panel) (arbitrary units). Dotted lines show the best-fitting Schechter functions. Error bars are computed using a bootstrapping technique.

Table 3. Group mass dependence of the LF in the $^{0.1}u$, $^{0.1}g$, $^{0.1}i$, and $^{0.1}z$ bands: STY best-fitting Schechter parameters

Mass sample ^a	N_{galaxies}	$M^* - 5 \log(h)$	α
$^{0.1}u$ band			
\mathcal{M}_1	4067	-17.72 ± 0.06	-1.03 ± 0.07
\mathcal{M}_2	3727	-17.70 ± 0.06	-0.98 ± 0.08
\mathcal{M}_3	3025	-17.77 ± 0.06	-1.07 ± 0.10
\mathcal{M}_4	2220	-17.91 ± 0.09	-1.15 ± 0.12
\mathcal{M}_5	1460	-18.10 ± 0.09	-1.51 ± 0.12
\mathcal{M}_6	1008	-18.15 ± 0.09	-1.55 ± 0.14
$^{0.1}g$ band			
\mathcal{M}_1	6794	-19.42 ± 0.04	-0.93 ± 0.04
\mathcal{M}_2	7303	-19.49 ± 0.04	-0.91 ± 0.05
\mathcal{M}_3	6965	-19.57 ± 0.05	-0.95 ± 0.05
\mathcal{M}_4	6381	-19.77 ± 0.05	-1.13 ± 0.06
\mathcal{M}_5	5209	-19.90 ± 0.06	-1.27 ± 0.06
\mathcal{M}_6	4095	-20.12 ± 0.07	-1.41 ± 0.07
$^{0.1}i$ band			
\mathcal{M}_1	7559	-20.74 ± 0.05	-0.90 ± 0.04
\mathcal{M}_2	8842	-20.93 ± 0.05	-0.95 ± 0.04
\mathcal{M}_3	9266	-21.02 ± 0.04	-1.02 ± 0.04
\mathcal{M}_4	9457	-21.16 ± 0.05	-1.12 ± 0.05
\mathcal{M}_5	9060	-21.30 ± 0.05	-1.26 ± 0.05
\mathcal{M}_6	9528	-21.64 ± 0.05	-1.50 ± 0.05
$^{0.1}z$ band			
\mathcal{M}_1	6519	-21.01 ± 0.05	-0.87 ± 0.05

Table 3—Continued

Mass sample ^a	N_{galaxies}	$M^* - 5 \log(h)$	α
\mathcal{M}_2	7643	-21.20 ± 0.05	-0.91 ± 0.05
\mathcal{M}_3	7938	-21.28 ± 0.05	-0.98 ± 0.05
\mathcal{M}_4	8092	-21.43 ± 0.05	-1.09 ± 0.05
\mathcal{M}_5	7619	-21.57 ± 0.05	-1.23 ± 0.06
\mathcal{M}_6	7861	-21.87 ± 0.05	-1.45 ± 0.05

^aSee Table 2

Table 4. Group mass dependence of the LF in the $^{0.1}r$ band for Blue and Red sequences

Mass sample ^a	N_{galaxies}	$M^* - 5 \log(h)$	α
Blue sequence			
All masses	29896	-20.76 ± 0.03	-1.47 ± 0.03
\mathcal{M}_1	4542	-20.46 ± 0.08	-1.36 ± 0.04
\mathcal{M}_2	4820	-20.45 ± 0.07	-1.35 ± 0.05
\mathcal{M}_3	4922	-20.54 ± 0.07	-1.38 ± 0.06
\mathcal{M}_4	4804	-20.59 ± 0.09	-1.38 ± 0.07
\mathcal{M}_5	4514	-20.64 ± 0.07	-1.33 ± 0.09
\mathcal{M}_6	5785	-21.08 ± 0.07	-1.62 ± 0.08
Red sequence			
All masses	53941	-20.85 ± 0.02	-0.87 ± 0.02
\mathcal{M}_1	5776	-20.29 ± 0.04	-0.53 ± 0.03
\mathcal{M}_2	7680	-20.50 ± 0.05	-0.63 ± 0.03
\mathcal{M}_3	8655	-20.60 ± 0.04	-0.70 ± 0.04
\mathcal{M}_4	9608	-20.80 ± 0.04	-0.85 ± 0.04
\mathcal{M}_5	10110	-20.98 ± 0.05	-1.00 ± 0.04
\mathcal{M}_6	11544	-21.36 ± 0.05	-1.27 ± 0.04

^aSee Table 2

Table 5. LF of galaxies in groups splitted by the difference in magnitude between the brightest and the second brightest galaxy

ΔM_{12}	Redshift range	N_{galaxies}	$M^* - 5 \log(h)$	α
≥ 0.6	0.02 – 0.05	6447	-20.8 ± 0.1	-1.14 ± 0.03
< 0.6	0.02 – 0.05	6553	-20.12 ± 0.06	-0.83 ± 0.03